Alterations to the bending mechanical properties of *Pinus sylvestris* timber according to flatwise and edgewise directions and knot position in the cross-section

Álvaro Fernández-Serrano[1] https://orcid.org/0000-0002-5171-5044♣
Antonio Villasante[1] https://orcid.org/0000-0002-7549-7424

[1]University of Lleida. School of Agrifood and Forestry Science and Engineering. Department of Agricultural and Forest Engineering. Lleida, Spain.

♣Corresponding author: alvaro.fernandezserrano@udl.cat

Abstract:
Given the heterogeneity of the material, the behaviour of a timber beam may differ depending on which of its sides is subjected to tension and which one is subjected to compression. An analysis is undertaken in the present work of the behaviour in non-destructive bending tests on the four sides of 57 samples of *Pinus sylvestris* (scots pine) of structural size ($2000 \times 100 \times 70$ mm^3). A study is additionally performed of the influence of the size and position of knots in the cross-section. The modulus of elasticity in flatwise direction was found to be 3 % higher than in edgewise direction. This difference could be attributable to the shear effect. While the introduction of knottiness variables did not improve modulus of elasticity prediction, it did decrease the error in the prediction of the modulus of rupture. The margin knot area ratio corresponding to the outer eighth of the cross-section's width occupied by knots was the knottiness variable with the lowest error in modulus of rupture prediction.

Introduction

Various authors have investigated the mechanical properties of scots pine (*Pinus sylvestris* L.) timber

through bending tests in order to know the modulus of elasticity (MOE) and the modulus of rupture

(MOR) (Arriaga *et al*. 2012, Krzosek *et al*. 2021, Ranta-Maunus *et al*. 2011). Bending tests have been

complemented with different non-destructive testing (NDT) techniques, including the vibration test

(Arriaga *et al*. 2012, Hassan *et al*. 2013, Villasante *et al*. 2019). In this way, the stiffness and bending strength could be easily predicted.

Some studies on conifers have attempted to improve the prediction of mechanical properties made with NDT by adding different variables related to the features of sawn timber. Ranta-Maunus *et al*. (2011) in scots pine (*Pinus sylvestris* L.) and Simic *et al*. (2019) in sitka spruce (*Picea sitchensis* ((Bong.) Carr.) studied the influence of density. Guntekin *et al*. (2013) in calabrian pine (*Pinus brutia* Ten.) and Martins *et al*. (2017) in cluster pine (*Pinus pinaster* Aiton) studied the relationship between rate of growth and mechanical properties. Arriaga *et al*. (2007) studied the influence of wanes in scots pine (*Pinus sylvestris* L.), and Arriaga *et al*. (2014) the effect of the slope of grain in radiata pine (*Pinus radiata* D. Don). Knottiness is one of the features with an important influence on the mechanical properties. This relationship has been studied in different works using scots pine (*Pinus sylvestris* L.). Conde García *et al*. (2007) used measurement of the relative diameter of the maximum knots on the face and on the edge. They verified that the inclusion of a knottiness variable improved MOE and MOR predictions made using models based exclusively on ultrasound speed. Hautamäki *et al*. (2014) found that MOR prediction from the MOE improved if the knot area ratio (KAR) was included in the model. Likewise, they found that MOE prediction on the basis of density improved when including KAR in the model. Arriaga *et al*. (2012) and Villasante *et al*. (2019) also used a similar measure of knottiness, the concentrated knot diameter ratio (CKDR). In both cases, the authors observed that adding the CKDR improved the prediction of MOR based on the longitudinal resonant frequency.

Some works have studied the influence of the position of knots along the piece. Baillères *et al*. (2012), in four-point bending tests using radiata pine (*Pinus radiata* D. Don), found that only the knots situated between the internal loading points had a significant contribution in the prediction of MOR. Wright *et al*. (2019), in tests with loblolly pine (*Pinus taeda* L.), found that the best MOE prediction was obtained when including only the knots that were within 85 % of the span and that the best MOR prediction was obtained with the knots located in 65 % of the span.

In contrast, very few works have studied the influence of the position of knots in the cross-section (tension or compression zones). In these cases, the margin knot area ratio (MKAR) was used, which is included in BS 4978 (2017). The margin zone used was a quarter of the width in the upper and lower margins. Lam *et al*. (2005), in tests made with douglas fir (*Pseudotsuga menziesii* (Mirb.), found that the MKAR could be used to establish grades for Canadian Douglas fir timber. Algin (2019) performed a multivariate optimisation on machine graded scaffold boards from sitka (*Picea sitchensis*, (Bong.) Carr.) including the KAR and MKAR simultaneously. In order to predict the mechanical characteristics of norway spruce (*Picea abies* (L.) H. Karst.), Lukacevic *et al*. (2015) constructed linear multivariate models that included some knot position measurements in the cross-section. Guindos and Guaita (2014) performed a theoretical simulation based on the characteristics of scots pine (*Pinus sylvestris* L.) timber to determine the influence of knot type and size, as well as its position in the cross-section. Their theoretical models indicated that the highest MOR decrease was due to the presence of margin knots (the knots most distant from the centre of the cross-section). As wood is a heterogenous and anisotropic material, the choice of the tension side in the bending test can have a significant effect on the mechanical properties. This is important when comparisons are made of results obtained by machine grading performed with a continuous lumber tester with those obtained through conventional bending tests. In the first case the samples are normally bent flatwise, whereas in the second the bending is commonly performed in edgewise direction. For this reason, it is of fundamental importance to know the relationship between the results of the tests in the two directions. Despite this, only very few works have studied this relationship. Some authors have found a high correlation between the MOE values calculated via bending in edgewise and flatwise directions. These include Kim *et al*. (2010) in southern pine ($R^2 = 0,69$), Baillères *et al*. (2012) in radiata pine (*Pinus radiata* D. Don) ($R^2 = 0,70$), Yang *et al*. (2015) in different conifers ($R^2 = 0,85$) and Pošta *et al*. (2016) in norway spruce (*Picea abies* (L.) H. Karst.) ($R^2 = 0,88$). Baillères *et al*. (2012) obtained a weak relationship ($R^2 = 0,41$) for the multiple linear regression with the MOE in flatwise direction and knottiness to predict the MOR in edgewise direction.

The aims of the present study were (1) to analyse the mechanical properties obtained via edgewise and flatwise bending tests in samples of scots pine (*Pinus sylvestris* L.), and (2) to verify whether the variables that take into account knot position in the cross-section can improve prediction of the mechanical bending properties calculated in both directions. Grading of scots pine (*Pinus sylvestris* L.) timber from the Montsec mountains (Spain) was not an objective of this work.

Materials and methods

Materials

The study was carried out using 57 samples of scots pine (*Pinus sylvestris* L.) with a size of 70 x 100 x 2000 mm^3 obtained from the province of Lerida (NE Spain). The pieces were selected randomly from a batch of unclassified timber at a local sawmill. Each sample was marked with a number. Each of the four sides was marked with a letter, A and C for the edges and B and D for the faces (Figure 1). The wood was stored for 10 months in the interior of a test laboratory until reaching constant weight (maximum difference of ± 0,1 % between weightings made with a time interval of 6 h) in accordance with EN 408:2011+A1 (2012). The same standard was used to measure each sample to obtain the density. The slope of grain and the rate of growth of each sample were measured in accordance with the procedure outlined in EN 1309-3 (2018).

Bending tests

The samples were subjected to a non-destructive four-point bending test using a 50-kN universal testing machine (Cohiner, Spain) to know the global MOE in accordance with EN 408:2011+A1 (2012). The test was performed four times, placing the loading heads on each of the four sides of the sample (Figure 1) to obtain four positional global MOE values (MOE$_A$, MOE$_B$, MOE$_C$, MOE$_D$). On the basis of these values, the mean MOE values in edgewise direction (MOE$_{edge}$, from MOE$_A$ and MOE$_C$) and in flatwise direction (MOE$_{flat}$ from MOE$_B$ and MOE$_D$) were obtained. For this test, a linear displacement transducer with spring (AEP Transducers, Italy) was used situated on the lower part of the piece. The distance between supports (1800 mm) was the same for the tests in edgewise and flatwise direction, and so the length-to-depth ratio was 18 and 25,7, respectively. The MOE was calculated with Equation 1 (EN 408:2011+A1 2012) using the stress-strain curve in the loading area between 10 % and 40 % of the estimated ultimate bending strength. It was verified that the linear regression presented an R^2 value above 0,99 for all the samples.

$$MOE = \frac{3aL^2 - 4a^3}{2bh^3\left(2\frac{\Delta w}{\Delta F} - \frac{6a}{5Gbh}\right)} \quad (1)$$

Where MOE is the modulus of elasticity, L is the distance between supports, a is the distance between the loading heads, b and h are the width and the depth of the sample, Δw is the increase in deformation, ΔF is the increase in force and G is the shear modulus. As allowed in EN 408:2011+A1 (2012), the shear effect was ignored taking a value G equal to infinity.

Test with other values of G were made in Equation 1 to analyse the influence of the shear effect on MOE$_{edge}$ and MOE$_{flat}$. Firstly, 650 MPa was used as also permitted in EN 408:2011+A1 (2012). A value of G equal to the MOE divided by 16 was also considered (EN 338 2016). A value of G equal to the MOE divided by 17 was then used, as proposed by Brancheriau *et al*. (2002). Finally, a value

of *G* was calculated to make both MOE values (MOE$_{edge}$ and MOE$_{flat}$) equal. These three values of *G* were obtained by iterative calculation.

The samples were also subjected to a destructive four-point bending test in edgewise direction to determine the MOR in accordance with EN 408:2011+A1 (2012). In this case, a different displacement transducer (Burster, Germany) was used situated on the mid-point of the side subjected to tension. The loading heads were always positioned on side A (Figure 1) until rupture to obtain the MOR$_A$. In this test, another global MOE value was also obtained (MOE$_{AR}$). The MOE$_A$ and MOE$_{AR}$ values should be identical but may present slight differences as two different displacement transducers were used and the wood was repositioned between both bending tests (destructive and non-destructive). The MOE$_{AR}$ was used as reference to analyse MOE variability according to the side on which the test was performed.
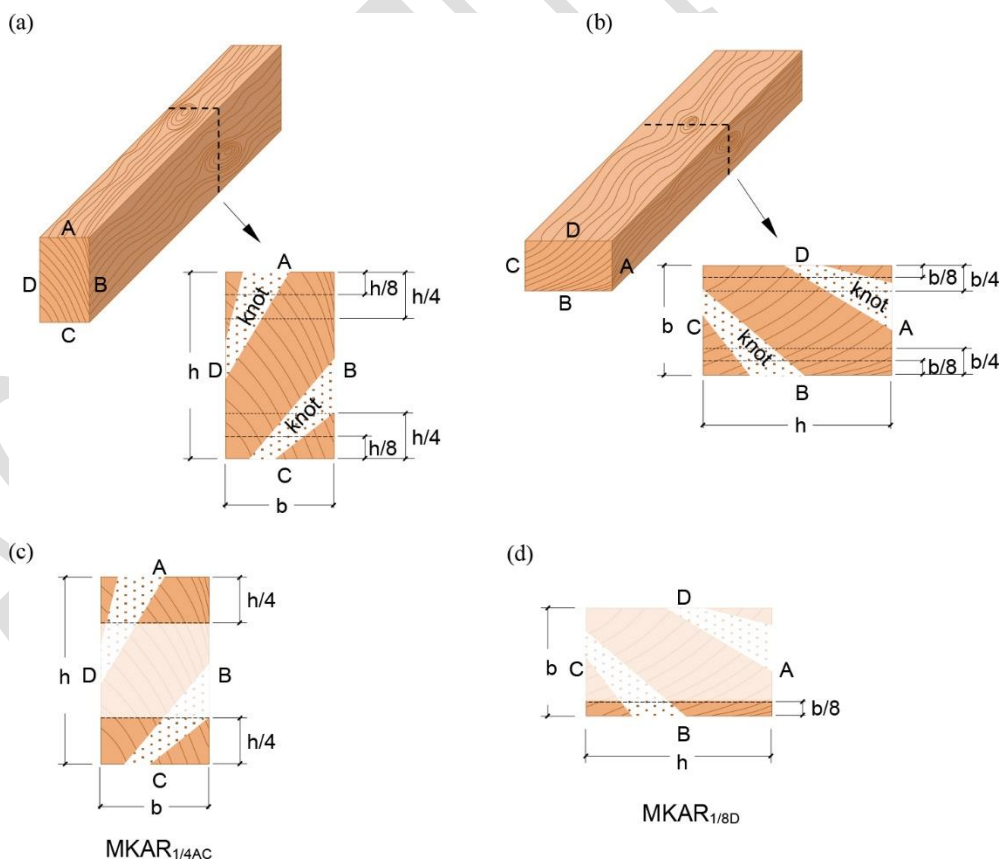
Figure 1: Knottiness measures based on the KAR: (a) Cross-section, edgewise direction, (b) Cross-section, flatwise direction, (c) example of MKAR$_{1/4}$, proportion of the margin cross-section (h/4) occupied by knots when the sample was tested in edgewise direction (loading heads on A), (d)

example of $MKAR_{1/8}$, proportion of the margin cross-section of tension (b/8) occupied by knots when the sample was tested in flatwise direction (loading heads on D).

The final moisture content (MC) of each sample was measured immediately after the bending tests with the oven dry method at 103 °C in accordance with EN 13183-1 (2002). No adjustments were made based on MC because all of the samples presented similar MC values and all the tests for each sample were conducted within an interval of less than one hour.

Knottiness

Two different criteria were followed to measure knottiness (Appendix 1). In the first approach, the width of each knot was measured in the direction perpendicular to the length of the piece in accordance with Annex A of EN 1309-3 (2018). Two variables were obtained from this measurement, $knot_{tot}$ when the sum of all the knots of the sample was included, and $knot_{1/3}$ when only the knots situated in the central third of the sample were included. The second approach used (Figure 1) was based on the knot area ratio (KAR) that indicates the proportion of the complete cross-section occupied by knots (Walker 1993). The margin knot area ratio (MKAR), that indicates the proportion of the margin cross-section occupied by knots, was used to determine the influence of the position of the knots with respect to the direction of the load. The MKAR allowed variables of positional knottiness to be obtained.

The $MKAR_{1/4}$ (BS 4978 2017) was measured, using as margin the outer quarter of the cross-section's width. The $MKAR_{1/8}$ was also measured, using as margin the outer eighth of the cross-section's width. The MKAR (Figure 1) were measured considering the direction of the bending test (edgewise or flatwise). In addition, it was also considered if the margin area was subjected to tension or compression. In this way, a total of 12 different MKAR-based measures of positional knottiness were obtained (Appendix 1).

Statistical analyses

The prediction was studied through simple linear regression (SLR) of the MOE_{AR} and MOR_A on the basis of each of the 12 variables of knottiness (Appendix 1) and the four positional MOE (MOE_A, MOE_B, MOE_C, and MOE_D). This first calculation allowed selection of the knottiness variables with the best predictive capacity. Attempts were then made to improve the predictive capacity of the SLR models using multiple linear regression (MLR) models of two variables. These models comprised a positional MOE and a knottiness variable.

The root-mean-square error (RMSE) was used instead of the coefficient of determination (R^2), commonly used in most previous studies, to assess the goodness-of-fit of the different models. This decision was adopted because it is more important to know the precision of the values generated by a model (RMSE) than to quantify the variability (R^2) of the predicted values (Alexander *et al*. 2015, Mansfield *et al*. 2007). Nonetheless, the R^2 value was also calculated to enable a comparison of the results obtained with those of other authors.

The models obtained from the whole dataset can be affected by overfitting because they are also fitted to the noise of the sample. For small datasets, the K-fold cross-validation can help avoid overfitting (Lever *et al*. 2016). In the present study, the 10-fold cross-validation method (Faydi *et al*. 2017, Hashim *et al*. 2016, Villasante *et al*. 2019) was used to calculate the RMSE of each model. The samples were randomly split into 10 groups of folds, using each group to validate the model generated with the remaining 9. This procedure was repeated 5 times to obtain 50 RMSE values for each model. WEKA 3.6 software (Waikato University 2014) was used to carry out this process. For the purposes of comparison with other studies, the 10-fold cross-validation was not applied in the calculation of R^2.

The non-parametric Kruskal-Wallis test was used to compare the RMSE values of each model. If statistically significant differences between the RMSE were found, a post hoc analysis was carried out using Dunn's test with Bonferroni adjustment. The Kruskal-Wallis test and post hoc analysis were performed with R 3.6.1 software (R Core Team 2019). In all cases, the level of significance was 0,05.

Results and discussion

MC, slope of grain, rate of growth and density of the samples are shown in Table 1. The differences in MC between samples were small. Pith was observed in just 12 % of samples.

Table 1: Characteristics of the samples.

Variable	Units	Mean value	SD	CV (%)
MC	%	11,3	0,67	5,90
Density	kg/m³	550	38,9	7,1
Slope of grain	%	5,2	3,47	66,7
Rate of growth	mm	3,2	0,77	23,8

MOE, MOR and knottiness values observed in the samples are shown in Table 2. The mean MOE values obtained for the different sides ranged between 7600 and 7900 MPa. These values were slightly lower than those observed by other authors in scots pine (*Pinus sylvestris* L.) (Arriaga *et al*. 2012, Krzosek *et al*. 2021, Ranta-Maunus *et al*. 2011). This can be attributed to the fact that in the present study unclassified structural timber was used.

In the case of the MOR a mean value of 40,0 MPa was obtained, similar to that obtained in other studies with scots pine (*Pinus sylvestris* L.) in Spain (Arriaga *et al*. 2012, Villasante *et al*. 2019). As for knottiness, a mean KAR value of 0,24 was obtained with high coefficient of variation (CV) values. This high variability between samples was a consequence of the random selection of unclassified

samples. Similar KAR values were observed by Hautamäki *et al*. (2014) in scots pine (*Pinus sylvestris* L.) (from 0,17 to 0,29), Hautamäki *et al*. (2013) in norway spruce (*Picea abies* (L.) H. Karst.) (from 0,17 to 0,21) and Steffen *et al*. (1997) in norway spruce (*Picea abies* (L.) H. Karst.) (from 0,17 to 0,24). For the different MKAR-related variables, values of around 0,25 were also obtained with a very high variability.

Table 2: Summary of the study variables.

Variable	Units	Mean value	SD	CV (%)
$knot_{1/3}$	mm	78	61	78,2
$knot_{tot}$	mm	283	166	58,7
KAR	$mm^2 \cdot mm^{-2}$	0,24	0,17	70,8
$MKAR_{1/4A}$	$mm^2 \cdot mm^{-2}$	0,27	0,25	92,6
$MKAR_{1/4B}$	$mm^2 \cdot mm^{-2}$	0,22	0,23	104,5
$MKAR_{1/4C}$	$mm^2 \cdot mm^{-2}$	0,23	0,26	113,0
$MKAR_{1/4D}$	$mm^2 \cdot mm^{-2}$	0,26	0,24	92,3
$MKAR_{1/4AC}$	$mm^2 \cdot mm^{-2}$	0,25	0,20	80,0
$MKAR_{1/4BD}$	$mm^2 \cdot mm^{-2}$	0,24	0,17	70,8
$MKAR_{1/8A}$	$mm^2 \cdot mm^{-2}$	0,28	0,26	92,9
$MKAR_{1/8B}$	$mm^2 \cdot mm^{-2}$	0,21	0,23	109,5
$MKAR_{1/8C}$	$mm^2 \cdot mm^{-2}$	0,23	0,27	117,4
$MKAR_{1/8D}$	$mm^2 \cdot mm^{-2}$	0,27	0,26	96,3
$MKAR_{1/8AC}$	$mm^2 \cdot mm^{-2}$	0,26	0,20	76,9
$MKAR_{1/8BD}$	$mm^2 \cdot mm^{-2}$	0,24	0,18	75,0
MOE_A	MPa	7701	1838	23,9
MOE_B	MPa	7879	2038	25,9
MOE_C	MPa	7647	1829	23,9
MOE_D	MPa	7869	1998	25,4
MOE_{edge}	MPa	7674	1829	23,8
MOE_{flat}	MPa	7874	2011	25,5
MOE_{AR}	MPa	7717	1849	24,0
MOR_A	MPa	40,0	15,6	39,0

Comparison of MOE_{flat} and MOE_{edge}

The MOE$_{flat}$ value was 2,6 % higher than the MOE$_{edge}$ value (Table 3). This difference can be attributed to the shear effect. When the deformation is measured over the entire length of the beam (global MOE), deformations due to shear are included in the total measured deformation (Boström 1999). In consequence, for both MOE$_{flat}$ and MOE$_{edge}$, in reality an apparent value was obtained that underestimated the true MOE value. The shear effect increases as the length-to-depth ratio decreases (Timoshenko 1938), which explains how MOE$_{flat}$ was higher than MOE$_{edge}$ (length-to-depth ratio of 25,7 and 18, respectively). The shear effect is especially important in wood because the MOE/G ratio is particularly high in comparison with an isotropic elastic material (Brancheriau *et al*. 2002). These results coincide with those of Kim *et al*. (2010) who, in three pine species of Korea, also found that MOE$_{flat}$ was higher than MOE$_{edge}$ (between 1,3 % and 6,1 %). These authors used a length-to-depth ratio in flatwise direction between 23 % and 45 % higher than in edgewise direction. This length-to-depth ratio value was similar to that of the present study (25,7 %), which explains the similar relationships between the MOE values. However, Boström (1994) and Steffen *et al*. (1997) obtained the opposite result in norway spruce (*Picea abies* (L.) H. Karst.), with MOE$_{flat}$ between 20 % and 40 % lower than MOE$_{edge}$. This discrepancy can be put down to two reasons. Firstly, these authors used different spans for the different bending directions, and so the length-to-depth ratio in flatwise direction was up to 30 % lower than in edgewise direction. With this arrangement, the shear effect caused an increase in the underestimation of the MOE in flatwise direction. Secondly, these authors used a four-point bending test in edgewise direction and a three-point bending test in flatwise direction. Brancheriau *et al.* (2002) found that a three-point bending test underestimates by about 19 % the MOE value in relation to a four-point loading test.

The differences detected between MOE$_{flat}$ and MOE$_{edge}$ should be considered when the pieces are classified by bending tests in flatwise direction and are subsequently installed in the structure in edgewise direction. Currently, classification is commonly made on the basis of flatwise direction tests because less loading is required to deform the pieces, as is the case of continuous lumber testers.

The MOE_{edge} and MOE_{flat} results with the different tested G values are shown in Table 3. When the shear effect is ignored ($G = \infty$) higher differences between both MOE are found. The value of 650 MPa proposed in EN 408:2011+A1 (2012) decreased the differences, but does not seem to be an appropriate value as it is a generic value for any MOE value and any species of softwood. Lower differences between MOE_{edge} and MOE_{flat} were observed with a G value equal to the MOE divided by 16 (EN 338 2016) and divided by 17 (Brancheriau *et al*. 2002). The differences between MOE_{edge} and MOE_{flat} disappeared for a G value equal to the MOE divided by 18,2. All indications are that the differences between the MOE_{edge} and MOE_{flat} values were due to shear effect differences caused by modifications to the length-to-depth ratio. In addition to this effect, other authors found that some features could influence in the relationship between MOE_{edge} and MOE_{flat}, such as knots and the slope of grain (Guindos and Ortiz 2013). To confirm the shear effect, it would be advisable to carry out tests with samples of other species and different length-to-depth ratios.

Table 3: MOE_{flat} and MOE_{edge} according to different G values.

G (MPa)	MOE_{edge} (MPa)	MOE_{flat} (MPa)	Increase of MOE_{flat} with respect to MOE_{edge}
∞ [1]	7674	7874	+ 2,61 %
650 [1]	7946	8012	+ 0,83 %
503 [2]	8028	8053	+ 0,31 %
474 [3]	8051	8065	+ 0,17 %
444 [4]	8078	8078	0

[1]Proposed by EN 408:2011+A1 (2012), [2]Proposed by EN 338 (2016), [3]Proposed by Brancheriau *et al*. (2002), [4]Value of G that makes both MOE values equal, [2,3,4]G values obtained by iterative calculation.

Selection of knottiness variables for MOE and MOR prediction

The predictive capacity of mechanical characteristics on the basis of knottiness variables is shown in Table 4. In the MOE_{AR} prediction, the lowest RMSE value was obtained with $knot_{1/3}$ and $knot_{tot}$, the

two knot variables based on EN 1309-3 (2018). These knot measures achieved better predictions than the local measures associated to KAR. The explanation for this is that the MOE values the global behaviour of the piece. The $knot_{1/3}$ variable obtained the lowest RMSE value because the highest bending moment values in the four-point bending test are given in the central third of the piece.

As for the MOR_A, the lowest RMSE values were obtained with $MKAR_{1/8AC}$. This shows that the knots situated in the tension and compressions margins are those which have the highest influence on rupture because this is where the highest bending stress values are found.

The R^2 values obtained in the prediction of the MOR_A on the basis of knottiness variables were higher than those obtained in the MOE_{AR} prediction (Table 4), which concurs with the observations of other authors in scots pine (*Pinus sylvestris* L.) (Conde García *et al.* 2007, Šilinskas *et al.* 2020) and in other pine species (Conde García *et al.* 2007, França *et al.* 2019, Wright *et al.* 2019). Only in one study was the opposite trend observed (Hautamäki *et al.* 2013, Hautamäki *et al.* 2014).

Table 4: Simple linear regression based on knottiness to predict MOE_{AR} and MOR_A.

	MOE_{AR}		MOR_A	
	RMSE (MPa)	R^2	RMSE (MPa)	R^2
$knot_{1/3}$	1458	0,37	11,59	0,45
$knot_{tot}$	1538	0,30	10,59	0,51
KAR	1671	0,16	10,81	0,51
$MKAR_{1/4A}$	1783	0,04	11,45	0,45
$MKAR_{1/4B}$	1728	0,08	13,39	0,23
$MKAR_{1/4C}$	1700	0,11	13,75	0,20
$MKAR_{1/4D}$	1744	0,11	13,39	0,26
$MKAR_{1/4AC}$	1706	0,12	10,61	0,53
$MKAR_{1/4BD}$	1644	0,18	11,22	0,48
$MKAR_{1/8A}$	1803	0,01	12,04	0,39
$MKAR_{1/8B}$	1711	0,11	13,28	0,24
$MKAR_{1/8C}$	1677	0,15	13,23	0,26
$MKAR_{1/8D}$	1757	0,11	14,02	0,20
$MKAR_{1/8AC}$	1714	0,11	10,09	0,57
$MKAR_{1/8BD}$	1618	0,21	11,80	0,42

RMSE calculated with the mean value of the 50 RMSE values (10-fold cross-validation, 5 repetitions); R^2 calculated with the whole dataset.
Lowest RMSE values shown in bold.

Linear regression to predict the MOE

Table 5 shows the predictive capacity of the MOE_{AR} (reference MOE) obtained on the basis of the four positional MOE (MOE_A, MOE_B, MOE_C, MOE_D). With respect to the differences between the four sides, MOE_A was the best MOE_{AR} predictor, which was expected as, although the sample was repositioned, the loading heads were positioned on the same side. MOE_B and MOE_D, both carried out in flatwise direction, obtained the worst prediction result, almost doubling the RMSE obtained with MOE_A. The explanation for this difference is that the test taken as reference (MOE_{AR}) corresponds to the edgewise direction.

It was also observed that adding a knottiness variable to any of the positional MOE did not improve MOE_{AR} prediction, and so the multivariable models offered no advantage. França *et al*. (2020) in southern pine and Wright *et al*. (2019) in loblolly pine (*Pinus taeda* L.) also found that introducing a knottiness variable in an MLR together with the dynamic MOE did not improve the prediction of the static MOE.

Table 5: RMSE of the linear regression to predict MOE_{AR}.

Variable	RMSE (MPa)	ΔRMSE [1] (%)
$1{,}00001 \times MOE_A + 15{,}39$	194,0 a	+0,2
$1{,}00364 \times MOE_A + 0{,}17577 \times knot_{1/3} - 26{,}23$	197,3 a	+1,9
$1{,}01683 \times MOE_A + 0{,}32321 \times knot_{tot} - 205{,}70$	193,7 a	−
$0{,}8904 \times MOE_B + 701{,}68$	341,2 bcd	+76,1
$0{,}85951 \times MOE_B - 1{,}76229 \times knot_{1/3} + 1082{,}51$	331,7 bcd	+71,2
$0{,}87864 \times MOE_B - 0{,}26483 \times knot_{tot} + 869{,}52$	342,4 bcd	+76,8
$0{,}99975 \times MOE_C + 72{,}26$	270,2 bc	+39,5
$0{,}99310 \times MOE_C - 0{,}32417 \times knot_{1/3} + 148{,}32$	274,5 bc	+41,7
$1{,}01940 \times MOE_C + 0{,}37190 \times knot_{tot} - 183{,}37$	268,7 b	+38,7
$0{,}90585 \times MOE_D + 588{,}90$	368,7 d	+90,3
$0{,}87478 \times MOE_D - 1{,}72791 \times knot_{1/3} + 967{,}97$	360,5 cd	+86,1
$0{,}88466 \times MOE_D - 0{,}47838 \times knot_{tot} + 891{,}16$	362,4 cd	+87,1

MOE in MPa, $knot_{1/3}$, and $knot_{tot}$ in mm
RMSE calculated with the mean value of the 50 RMSE values (10-fold cross-validation, 5 repetitions)
The same letter indicates there are no statistically significant differences (Kruskal-Wallis test, post hoc Dunn's test with Bonferroni adjustment)
[1] RMSE increase with respect to the model with the lowest error

Linear regression to predict the MOR

Table 6 shows the predictive capacity of the MOR obtained on the basis of the four positional MOE and the knottiness variables. No statistically significant differences were found between the MOR predictions made through SLR on the basis of any of the four positional MOE. Inclusion in the model of the $knot_{tot}$ variable did give improvements to the prediction but these were not statistically significant. The situation changed when including $MKAR_{1/8}$ in the model as a knottiness variable. When adding this variable, the two tests performed in edgewise direction predicted MOR with a statistically significant lower RMSE (around 48 %) than that of the tests in flatwise direction. The R^2 value also improved, with an increase of 0,30. However, this reduction in the error was clearly lower in flatwise direction.

Table 6: Linear regression to predict the MOR_A.

Model	RMSE (MPa)	ΔRMSE [1] (%)	R^2
$0,00561 \times MOE_A - 3,21$	11,71 c	+48,8	0,44
$0,00383 \times MOE_A - 45,6 \times MKAR_{1/8AC} + 22,2$	7,93 ab	+0,8	0,75
$0,00322 \times MOE_A - 0,0461 \times knot_{tot} + 28,3$	10,09 bc	+28,2	0,60
$0,00491 \times MOE_B + 1,37$	11,99 c	+52,4	0,41
$0,00337 \times MOE_B - 39,8 \times MKAR_{1/8BD} + 23,1$	10,41 c	+32,3	0,57
$0,00277 \times MOE_B - 0,0480 \times knot_{tot} + 31,8$	10,13 c	+28,7	0,60
$0,00571 \times MOE_C - 3,62$	11,61 c	+47,5	0,45
$0,00391 \times MOE_C - 45,3 \times MKAR_{1/8AC} + 21,7$	7,87 a	–	0,75
$0,00331 \times MOE_C - 0,0455 \times knot_{tot} + 27,6$	10,01 abc	+27,2	0,61
$0,00494 \times MOE_D + 1,19$	12,08 c	+53,5	0,40
$0,00340 \times MOE_D - 40,8 \times MKAR_{1/8BD} + 23,1$	10,38 c	+31,9	0,57
$0,00277 \times MOE_D - 0,0488 \times knot_{tot} + 32$	10,11 c	+28,5	0,59

MOE in MPa, MKAR in $mm^2 \cdot mm^{-2}$, $knot_{tot}$ in mm
RMSE calculated with the mean value of the 50 RMSE values (10-fold cross-validation, 5 repetitions); R^2 calculated with the whole dataset.
The same letter indicates there are no statistically significant differences (Kruskal-Wallis test, post hoc Dunn's test with Bonferroni adjustment)
[1]RMSE increase with respect to the model with the lowest error.

This trend concurred with that observed by other authors in scots pine (*Pinus sylvestris* L.) who also obtained improvements in MOR prediction on the basis of the MOE when introducing a knottiness variable in the model. None of the studies used positional variables of knottiness similar to the MKAR$_{1/8}$ used in the present study. Hautamäki *et al.* (2014) observed an RMSE reduction of 3 % and an R^2 increase of 0,05. Villasante *et al.* (2019) obtained an RMSE reduction of 6 % and an R^2 increase of 0,07. Arriaga *et al.* (2012) and Conde García *et al.* (2007) observed increases of 0,04 and 0,16, respectively, in the R^2 value. França *et al.* 2020, França *et al.* 2019 in southern pine and Wright *et al.* (2019) in loblolly pine (*Pinus taeda* L.) obtained an R^2 increase of between 0,05 and 0,17. In these studies, the R^2 increase when including a knottiness variable in the MOR prediction (between 0,04 and 0,17) was some distance from the 0,30 increase obtained in the present study. This result shows the advantage of using the positional knottiness variable MKAR$_{1/8}$ in the MOR prediction.

Conclusions

The MOE calculated in flatwise direction was higher than the MOE calculated in edgewise direction. The difference between the two values could be explained by the shear effect.

A ratio of 18 between the MOE and the shear modulus was obtained. This value is close to the ratio of 17 proposed by Brancheriau *et al.* (2002), the relationship found in previous works that best explained the differences between the flatwise and edgewise directions.

Knottiness measured in accordance with Annex A of EN 1309-3 (2018) was the best MOE predictor. However, the positional measures of knottiness which consider the position of knots in the cross-section were the most useful for MOR prediction. Of these positional measures, MKAR$_{1/8}$ produced the lowest error in MOR prediction.

No differences were found in MOR prediction in edgewise direction on the basis of the four positional MOE (MOE_A, MOE_B, MOE_C, and MOE_D). However, when including the positional variable $MKAR_{1/8}$ in the prediction, the MOE obtained in edgewise direction presented statistically significantly lower RMSE values than the MOE in flatwise direction.

The RMSE value in MOR prediction on the basis of the MOE decreased by 32,3 % when the positional knottiness variable $MKAR_{1/8}$ was added.

The differences between MOE_{edge} and MOE_{flat} should be considered when the wood is classified with a bending test in one direction and is installed in the structure in another direction.

Authorship contributions

A.F-S.: Conceptualization, data curation, formal analysis, investigation, methodology, resources, validation, visualization, writing - original draft preparation, writing - review & editing. A.V.: Conceptualization, data curation, formal analysis, investigation, methodology, resources, validation, writing - review & editing.

All authors have read and agreed to the published version of the manuscript.

References:
Alexander, D.L.J.; Tropsha, A.; Winkler, D.A. 2015. Beware of R2: Simple, Unambiguous Assessment of the Prediction Accuracy of QSAR and QSPR Models. *Journal of Chemical Information and Modeling* 55(7): 1316-1322. https://doi.org/10.1021/acs.jcim.5b00206.
Algin, Z. 2019. Multivariate performance optimisation of scaffold boards with selected softwood defects. *Construction and Building Materials* 220: 667-678. https://doi.org/10.1016/j.conbuildmat.2019.05.190
Arriaga, F.; Esteban, M.; Argüelles, R.; Bobadilla, I.; Íñiguez-González, G. 2007. The effect of wanes on the bending strength of solid timber beams. *Materiales de Construccion* 57(288): 61-76. https://doi.org/10.3989/mc.2007.v57.i288.65
Arriaga, F.; Iniguez-Gonzalez, G.; Esteban, M.; Divos, F. 2012. Vibration method for grading of large cross-section coniferous timber species. *Holzforschung* 66(3): 381-387. https://doi.org/10.1515/HF.2011.167
Arriaga, F.; Monton, J.; Segues, E.; Iniguez-Gonzalez, G. 2014. Determination of the mechanical properties of radiata pine timber by means of longitudinal and transverse vibration methods. *Holzforschung* 68(3): 299-305. https://doi.org/10.1515/hf-2013-0087
Baillères, H.; Hopewell, G.; Boughton, G.; Brancheriau, L. 2012. Strength and stiffness assessment technologies for improving grading effectiveness of radiata pine wood. *BioResources* 7(1): 1264-1282. https://doi.org/10.15376/biores.7.1.1264-1282

Boström, L. 1994. Machine strength grading. Comparison of four different systems. *Swedish National Testing and Research Institute*. SP Report 1994:49. http://ri.diva-portal.org/smash/get/diva2:961864/FULLTEXT01.pdf

Boström, L. 1999. Determination of the modulus of elasticity in bending of structural timber - Comparison of two methods. *Holz Als Roh - Und Werkst* 57(2): 145-149. https://doi.org/10.1007/s001070050030

Brancheriau, L.; Bailleres, H.; Guitard, D. 2002. Comparison between modulus of elasticity values calculated using 3 and 4 point bending tests on wooden samples. *Wood Science and Technology* 36(5): 367-383. https://doi.org/10.1007/s00226-002-0147-3

BS. 2017. Visual Strength Grading of Softwood. Specification. BS 4978-2007+A2-2017: London, UK.

Conde García, M.; Fernández-Golfín Seco, J.I.; Hermoso Prieto, E. 2007. Mejora de la predicción de la resistencia y rigidez de la madera estructural con el método de ultrasonidos combinado con parámetros de clasificación visual. Improving the prediction of strength and rigidity of structural timber by combining ultrasound techniques with visual grading parameters. *Materiales de Construccion* 57(288): 49-59. https://doi.org/10.3989/mc.2007.v57.i288.64

EN. 2002. Moisture content of a piece of sawn timber. Part 1: Determination by oven dry method. EN 13183-1-2002. Brussels, Belgium.

EN. 2012. Timber structures. Structural timber and glued laminated timber. Determination of some physical and mechanical properties. EN 408-2011+A1-2012. Brussels, Belgium.

EN. 2016. Structural timber. Strength classes. EN 338-2016. Brussels, Belgium.

EN. 2018. Round and sawn timber - Methods of measurements - Part 3: Features and biological degradations. EN 1309-3-2018: Brussels, Belgium.

Faydi, Y.; Brancheriau, L.; Pot, G.; Collet, R. 2017. Prediction of oak wood mechanical properties based on the statistical exploitation of vibrational response. *BioResources* 12(3): 5913-5927. https://doi.org/10.15376/biores.12.3.5913-5927

França, F.J.N.; França, T.S.F.A.; Seale, R.D.; Shmulsky, R. 2020. Use of longitudinal vibration and visual characteristics to predict mechanical properties of No. 2 southern pine 2x8 and 2x10 lumber. *Wood and Fiber Science* 52(3): 280-291. https://doi.org/10.22382/wfs-2020-026

França, F.J.N.; Seale, R.D.; Shmulsky, R.; França, T.S.F.A. 2019. Modeling mechanical properties of 2 by 4 and 2 by 6 southern pine lumber using longitudinal vibration and visual characteristics. *Forest Products Journal* 68(3): 286-294. https://meridian.allenpress.com/fpj/article/68/3/286/73763/Modeling-Mechanical-Properties-of-2-by-4-and-2-by

Guindos, P.; Guaita, M. 2014. The analytical influence of all types of knots on bending. *Wood Science and Technology* 48(3): 533-552. https://doi.org/10.1007/s00226-014-0621-8

Guindos, P.; Ortiz, J. 2013. The utility of low-cost photogrammetry for stiffness analysis and finite-element validation of wood with knots in bending. *Biosystems Engineering* 114(2): 86-96. https://doi.org/10.1016/j.biosystemseng.2012.11.002

Guntekin, E.; Emiroglu, Z.; Yilmaz, T. 2013. Prediction of bending properties for Turkish Red Pine (*Pinus brutia* Ten.) Lumber using stress wave method. *BioResources* 8(1): 231-237. http://dx.doi.org/10.15376/biores.8.1.231-237

Hashim, U.R.; Hashim, S.Z.M.; Muda, A.K. 2016. Performance evaluation of multivariate texture descriptor for classification of timber defect. *Optik* 127(15): 6071-6080. https://doi.org/10.1016/j.ijleo.2016.04.005

Hassan, K.T.S.; Horacek, P.; Tippner, J. 2013. Evaluation of stiffness and strength of scots pine wood using resonance frequency and ultrasonic techniques. *BioResources* 8(2): 1634-1645. http://dx.doi.org/10.15376/biores.8.2.1634-1645

Hautamäki, S.; Kilpeläinen, H.; Verkasalo, E. 2013. Factors and models for the bending properties of sawn timber from Finland and north-western Russia. Part I: Norway spruce. *Baltic Forestry* 19(1): 106-119. https://jukuri.luke.fi/handle/10024/517641

Hautamäki, S.; Kilpeläinen, H.; Verkasalo, E. 2014. Factors and models for the bending properties of sawn timber from Finland and north-western Russia. Part II: Scots pine. *Baltic Forestry* 20(1): 142-156. https://jukuri.luke.fi/handle/10024/518279

Kim, K.M.; Shim, K.B.; Lum, C. 2010. Predicting tensile and compressive moduli of structural lumber. *Wood and Fiber Science* 43(1): 83-89. https://wfs.swst.org/index.php/wfs/article/view/610

Krzosek, S.; Grześkiewicz, M.; Burawska-Kupniewska, I.; Mańkowski, P.; Wieruszewski, M. 2021. Mechanical properties of polish-grown *Pinus sylvestris* L. structural sawn timber from the butt, middle and top logs. *Wood Research* 66(2): 231-242. https://doi.org/10.37763/wr.1336-4561/66.2.231242

Lam, F.; Barrett, J.D.; Nakajima, S. 2005. Influence of knot area ratio on the bending strength of Canadian Douglas fir timber used in Japanese post and beam housing. *Journal of Wood Science* 51(1): 18-25. https://doi.org/10.1007/s10086-003-0619-6

Lever, J.; Krzywinski, M.; Altman, N. 2016. Points of Significance: Model selection and overfitting. *Nature Methods* 13(9): 703-704. https://doi.org/10.1038/nmeth.3968

Lukacevic, M.; Füssl, J.; Eberhardsteiner, J. 2015. Discussion of common and new indicating properties for the strength grading of wooden boards. *Wood Science and Technology* 49(3): 551-576. https://doi.org/10.1007/s00226-015-0712-1

Mansfield, S.D.; Iliadis, L.; Avramidis, S. 2007. Neural network prediction of bending strength and stiffness in western hemlock (*Tsuga heterophylla* Raf.). *Holzforschung* 61(6): 707-716. https://doi.org/10.1515/HF.2007.115

Martins, C.E.J.; Dias, A.M.P.G.; Marques, A.F.S.; Dias, A.M.A. 2017. Non-destructive methodologies for assessment of the mechanical properties of new utility poles. *BioResources* 12(2): 2269-2283. https://doi.org/10.15376/biores.12.2.2269-2283

Pošta, J.; Ptáček, P.; Jára, R.; Terebesyová, M.; Kuklík, P.; Dolejš, J. 2016. Correlations and differences between methods for non-destructive evaluation of timber elements. *Wood Research* 61(1): 129-140. http://www.woodresearch.sk/cms/correlations-and-differences-between-methods-for-non-destructive-evaluation-of-timber-elements/

R Core Team. 2019. R: A language and environment for statistical computing. Version 3.6.1. R Foundation for Statistical Computing: Vienna, Austria. https://www.r-project.org/

Ranta-Maunus, A.; Denzler, J.K.; Stapel, P. 2011. Strength of European timber. Part 2. Properties of spruce and pine tested in Gradewood project. VTT Technical Research Centre of Finland VTT Working Papers, No. 179. https://publications.vtt.fi/pdf/workingpapers/2011/W179.pdf

Šilinskas, B.; Varnagiryte-Kabašinskiene, I.; Aleinikovas, M.; Beniušiene, L.; Aleinikoviene, J.; Škema, M. 2020. Scots pine and Norway spruce wood properties at sites with different stand densities. *Forests* 11(5): 1-15. https://doi.org/10.3390/F11050587

Simic, K.; Gendvilas, V.; O'Reilly, C.; Harte, A.M. 2019. Predicting structural timber grade-determining properties using acoustic and density measurements on young Sitka spruce trees and logs. *Holzforschung* 73(2): 139-149. https://doi.org/10.1515/hf-2018-0073

Steffen, A.; Johansson, C.J.; Wormuth, E.W. 1997. Study of the relationship between flatwise and edgewise moduli of elasticity of sawn timber as a means to improve mechanical strength grading technology. *Holz Als Roh - Und Werkst* 55(4): 245-253. https://doi.org/10.1007/bf02990556

Timoshenko, S. 1938. Strength of materials. D. Van Mostrand Company, Inc.: New York, USA.

Villasante, A.; Iniguez-Gonzalez, G.; Puigdomenech, L. 2019. Comparison of various multivariate models to estimate structural properties by means of non-destructive techniques (NDTs) in *Pinus sylvestris* L. timber. *Holzforschung* 73(4): 331-338. https://doi.org/10.1515/hf-2018-0103

Waikato University. 2014. WEKA software. Version 3.6.12. Waikato University: Hamilton, New Zealand. https://ml.cms.waikato.ac.nz/weka/index.html

Walker, J. 1993. Primary Wood Processing: Principles and Practice. Chapman & Hall: London, UK.

Wright, S.; Dahlen, J.; Montes, C.; Eberhardt, T.L. 2019. Quantifying knots by image analysis and modeling their effects on the mechanical properties of loblolly pine lumber. Eur. *European Journal of Wood and Wood Products* 77(5): 903-917. https://doi.org/10.1007/s00107-019-01441-8
Yang, B.Z.; Seale, R.D.; Shmulsky, R.; Dahlen, J.; Wang, X. 2015. Comparison of nondestructive testing methods for evaluating no. 2 southern pine lumber: Part B, modulus of rupture. *Wood and Fiber Science* 47(4): 375-384. https://wfs.swst.org/index.php/wfs/article/view/2367

Appendix 1: Knottiness and MOE variables. Description

$knot_{tot}$	:	Sum of the cross dimensions of all the knots of the sample, in accordance with EN 1309-3
$knot_{1/3}$	:	As above, but only the knots found in the central third of the sample
KAR:	:	Knot Area Ratio, the proportion of the cross-section occupied by the knots
$MKAR_{1/4AC}$	:	The proportion of the margin cross section (outer quarters: h/4) occupied by the knots when the sample is tested in edgewise direction (loading heads situated on sides A or C)
$MKAR_{1/4BD}$	:	The proportion of the margin cross section (outer quarters: b/4) occupied by the knots when the sample is tested in flatwise direction (loading heads situated on sides B or D)
$MKAR_{1/4i}$	:	The proportion of the margin cross section occupied by the knots. Margin: outer quarter subjected to tension when the loading heads are situated on side i ($MKAR_{1/4A}$, $MKAR_{1/4B}$, $MKAR_{1/4C}$, $MKAR_{1/4D}$ for A, B, C, and D, respectively)
$MKAR_{1/8AC}$	:	The proportion of the margin cross section (outer eighth: h/8) occupied by the knots when the sample is tested in edgewise direction (loading heads situated on sides A or C)
$MKAR_{1/8BD}$	:	The proportion of the margin cross section (outer eighth: b/8) occupied by the knots when the sample is tested in flatwise direction (loading heads situated on sides B or D)
$MKAR_{1/8i}$	:	The proportion of the margin cross section occupied by the knots. Margin: outer eighth subjected to tension when the loading heads are situated on side i ($MKAR_{1/8A}$, $MKAR_{1/8B}$, $MKAR_{1/8C}$, $MKAR_{1/8D}$ for A,B, C, and D, respectively)
MOE_i	:	Global MOE. Loading heads situated on side i (i = A, B, C, or D)
MOE_{AR}	:	Global MOE obtained in the destructive bending test. Loading heads situated on side A
MOR_A	:	MOR in edgewise direction. Loading heads situated on side A